



HAL
open science

A putative function of the Arabidopsis Fe-phytosiderophore transporter homolog AtYSL2 in Fe and Zn homeostasis

G. Schaff, A. Schikora, J. Häberle, Grégory Vert, U. Ludewig, J.F. Briat,
Catherine Curie, N. von Wiren

► **To cite this version:**

G. Schaff, A. Schikora, J. Häberle, Grégory Vert, U. Ludewig, et al.. A putative function of the Arabidopsis Fe-phytosiderophore transporter homolog AtYSL2 in Fe and Zn homeostasis. *Plant and Cell Physiology*, 2005, 46, pp.762-774. 10.1093/pcp/pci081 . hal-00086935

HAL Id: hal-00086935

<https://hal.science/hal-00086935>

Submitted on 20 Dec 2020

HAL is a multi-disciplinary open access archive for the deposit and dissemination of scientific research documents, whether they are published or not. The documents may come from teaching and research institutions in France or abroad, or from public or private research centers.

L'archive ouverte pluridisciplinaire **HAL**, est destinée au dépôt et à la diffusion de documents scientifiques de niveau recherche, publiés ou non, émanant des établissements d'enseignement et de recherche français ou étrangers, des laboratoires publics ou privés.

A Putative Function for the *Arabidopsis* Fe–Phytosiderophore Transporter Homolog AtYSL2 in Fe and Zn Homeostasis

Gabriel Schaaf^{1,4}, Adam Schikora^{2,4}, Jennifer Häberle¹, Grégory Vert², Uwe Ludewig³, Jean-François Briat², Catherine Curie² and Nicolaus von Wirén^{1,5}

¹ Institut für Pflanzenernährung, Universität Hohenheim, D-70593 Stuttgart, Germany

² Biochimie et Physiologie Moléculaire des Plantes, Centre National de la Recherche Scientifique (Unité Mixte de Recherche 5004)/Institut National de la Recherche Agronomique/Agro-M/Université Montpellier II, 2 place Viala, F-34060 Montpellier cedex 1, France

³ ZMBP-Pflanzenphysiologie, Universität Tübingen, Auf der Morgenstelle 1, D-72076 Tübingen, Germany

Although *Arabidopsis thaliana* does not produce phytosiderophores (PS) under Fe deficiency, it contains eight homologs of the metal–PS/metal–nicotianamine (NA) transporter ZmYS1 from maize. This study aimed to investigate whether one of the closest *Arabidopsis* homologs to ZmYS1, AtYSL2, is involved in metal–chelate transport. Northern analysis revealed high expression levels of AtYSL2 in Fe-sufficient or Fe-resupplied roots, while under Fe deficiency transcript levels decreased. Quantitative real-time polymerase chain reaction (PCR) and analysis of transgenic plants expressing an AtYSL2 promoter:: β -glucuronidase gene further allowed the detection of down-regulated AtYSL2 gene expression under Zn and Fe deficiency. In contrast to ZmYS1, AtYSL2 did not mediate metal–PS or metal–NA transport in yeast mutants defective in Cu or Fe uptake, nor did AtYSL2 mediate Fe(II)–NA-, Fe(III)–NA- or Ni(II)–NA-inducible currents when assayed by two-electrode voltage clamp in *Xenopus* oocytes. Moreover, truncation of the N-terminus to remove putative phosphorylation sites that might trigger autoinhibition did not confer functionality to AtYSL2. A direct growth comparison of yeast cells transformed with AtYSL2 in two different yeast expression vectors showed that transformation with empty pFL61 repressed growth even under non-limiting Fe supply. We therefore conclude that the yeast complementation assay previously employed does not allow the identification of AtYSL2 as an Fe–NA transporter. Transgenic plants expressing an AtYSL2 promoter:: β -glucuronidase gene showed expression in root endodermis and pericycle cells facing the meta-xylem tubes. Taken together, our investigations support an involvement of AtYSL2 in Fe and Zn homeostasis, although functionality or substrate specificity are likely to differ between AtYSL2 and ZmYS1.

Keywords: nicotianamine — iron transport — strategy II — yeast complementation — *Xenopus* oocytes.

Abbreviations: DMA, 2'-deoxy-mugineic acid; GFP, green fluorescent protein; GUS, β -glucuronidase; NA, nicotianamine; NAAT, nicotianamine amino-transferase; NAS, nicotianamine synthase; ORF, open reading frame; PS, phytosiderophore; TMD, transmembrane-spanning domain.

⁴ These authors contributed equally to this work.

⁵ Corresponding author: E-mail, vonwiren@uni-hohenheim.de; Fax, +49-711-459-3295.

Introduction

Iron (Fe) is an essential element for all plants and plays a critical role in respiration, photosynthesis and many other cellular functions, including DNA synthesis and hormone production. Although abundant in the earth's crust, plant availability of Fe is extremely low in oxygenated environments due to the formation of low-soluble ferric hydroxide complexes at neutral or alkaline pH (Guerinot and Yi 1994).

In contrast, under anaerobic conditions, Fe, like other transition metals, can become toxic when hyper-accumulated or maldistributed within cells due to the generation of free radicals by Fenton chemistry (Briat and Lebrun 1999). Therefore, plants need to tightly control Fe uptake, intracellular compartmentation and distribution into the various plant organs (Briat and Lobréaux 1997, Wei and Theil 2000). In addition, due to deleterious effects of Fe(II), control of the Fe redox state and control of the biosynthesis of Fe chelators seem to be of particular importance for the cellular homeostasis of Fe.

Plants have developed two strategies to acquire Fe from soils under Fe-limiting conditions as first proposed by Römheld and Marschner (1986). In strategy I, which is found in dicots and non-graminaceous monocots, Fe has to be reduced prior to uptake. Therefore, proton secretion by plasma membrane H⁺-ATPases and reduction capacity as well as Fe(II) transport are enhanced under Fe-deficient growth conditions (Schmidt 2003). In contrast, in strategy II, as found in graminaceous plant species, Fe is chelated extracellularly by hexadentate chelators, so-called phytosiderophores (PS), and is subsequently taken up as intact Fe(III)–PS complexes. Both PS release and Fe(III)–PS uptake are enhanced under Fe deficiency, whereas the reduction-dependent pathway for Fe uptake remains in most cases constitutively expressed (Zaharieva and Römheld 2001, Bughio et al. 2002). In the past years, many of the mechanisms involved in Fe acquisition by strategy I and strategy II plants have been described at the molecular level (summarized in Curie and Briat 2003, Schmidt 2003). The genes encoding AtFRO2 and AtIRT1, that are mainly responsible for extracellular Fe reduction and Fe²⁺ uptake into roots in the strategy I plant *Arabidopsis*, have been isolated and the encoded proteins

characterized (Eide et al. 1996, Robinson et al. 1999). In strategy II, genes encoding nicotianamine synthase (NAS) and nicotianamine amino-transferase (NAAT), both key players in PS biosynthesis, as well as the high-affinity Fe(III)–PS transporter ZmYS1 have been isolated and the encoded proteins have been characterized (Higuchi et al. 1999, Takahashi et al. 1999, Curie et al. 2001, Schaaf et al. 2004). All these proteins are involved in Fe acquisition. In contrast, to date, only a few gene products are known that might play a role in intracellular transport of Fe and other heavy metals. For instance, AtNRAMP3 is localized to the tonoplast of root cells in the vascular bundle and might be involved in mobilizing vacuolar Fe, Zn and Mn to the cytoplasm (Thomine et al. 2003). Due to the presence of highly homologous *NRAMP* genes in both dicot and monocot plants, and the modulation of Cd and Fe toxicity by different members of the *NRAMP* family in plants, a more general function in metal homeostasis independent of the strategy for Fe acquisition has been postulated (Belouchi et al. 1997, Curie et al. 2000, Thomine et al. 2000, Mäser et al. 2001, Thomine et al. 2003).

For the chelation of Fe within plants, several potential ligands have been discussed. In the xylem, these are citrate for both strategy I and strategy II plants (Tiffin 1965). Moreover, in strategy II plants, mugineic acid and deoxy-mugineic acid, two PS species, may also chelate Fe in the xylem (Mori et al. 1987, Kawai et al. 2001). One of the most promising candidates for intracellular Fe chelation seems to be nicotianamine (NA). NA, a structural analog of PS and precursor of PS biosynthesis in graminaceous plant species, is present in all higher plants. Its critical function in Fe homeostasis is supported by the chlorotic phenotypes of the tomato mutant *chloronerva* and of NAAT-overexpressing tobacco, both of which have decreased levels of NA (Pich et al. 1994, Stephan et al. 1996, Takahashi et al. 2003).

NA has been shown to chelate Fe, Cu, Zn and Mn (Benes et al. 1983, Stephan and Scholz 1993, Stephan et al. 1996). The unexpected high kinetic stability of Fe(II)–NA and the low Fenton activity of Fe(II)–NA and Fe(III)–NA suggest that NA possesses an important function in scavenging Fe and protecting cells from oxidative damage (von Wirén et al. 1999). This function of NA has been corroborated by the observation that NA levels correlate with the amount and distribution of Fe in pea and tomato plants (Pich et al. 2001). Furthermore, the maize NAS gene *ZmNAS3* is induced under Fe-sufficient conditions and repressed under Fe deficiency (Mizuno et al. 2003), which provides evidence for an involvement of NA in Fe nutrition in grasses other than in PS biosynthesis. A first link between Fe chelation by NA and Fe transport across biological membranes has been made by the observation that the maize ZmYS1 protein mediates transport not only of Fe–PS and other metal–PS complexes (von Wirén et al. 1994, von Wirén et al. 1996, Curie et al. 2001, Schaaf et al. 2004) but also of Fe(II)–, Fe(III)– and Ni(II)–NA complexes as shown by heterologous expression in yeast and *Xenopus* oocytes (Schaaf et al. 2004). Since eight homologs of ZmYS1, named AtYSL1–8 (for ‘yel-

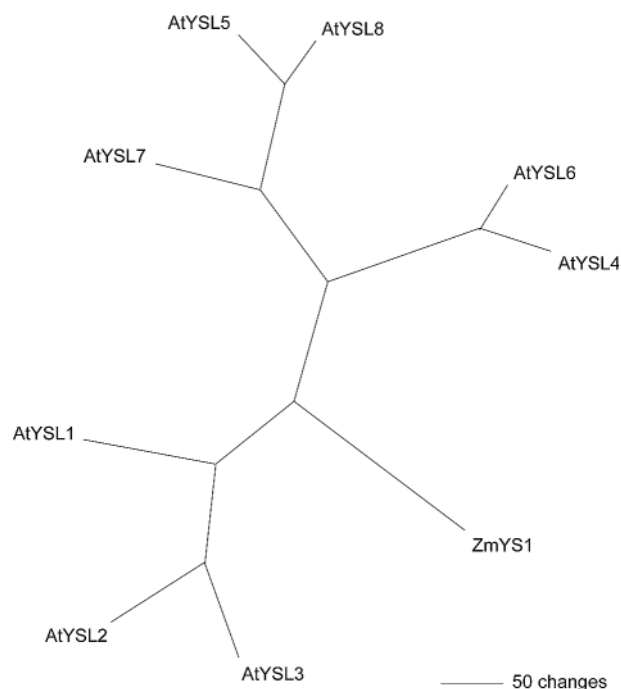


Fig. 1 Phylogenetic tree of YSL proteins. Unrooted, parsimony-based phylogram of ZmYS1 and the eight AtYSL homologs. Sequences have been aligned with Clustal W (Thompson et al. 1994) and submitted to the PAUP program, version 4.0 b5 (D. Swofford 1998, Smithsonian Institution, Washington, DC, USA). Bootstrap values of >50 are indicated (1,000 replicates, full heuristic search option, tree bisection reconnection branch swapping with random addition). The protein accession numbers used were: ZmYS1 (AAG17016), AtYSL1 (NP_567694), AtYSL2 (AY648977), AtYSL3 (NP_200167), AtYSL4 (NP_198916), AtYSL5 (NP_566584), AtYSL6 (NP_566806), AtYSL7 (NP_176750) and AtYSL8 (NP_564525).

low stripe-like’), have been found in the strategy I plant *Arabidopsis* (Curie et al. 2001), the question arose of whether these homologs might be involved in Fe–NA transport and contribute to Fe homeostasis.

In the present study, we describe several independent approaches to investigate whether AtYSL2, one of the closest homologs of ZmYS1, is involved in Fe nutrition or heavy metal homeostasis. Unlike ZmYS1, we could not observe that AtYSL2 restores growth of the yeast Fe uptake-defective mutant *fet3 fet4* in the presence of Fe–NA or Fe–PS chelates. However, expression analyses by Northern gel blots, real-time polymerase chain reaction (PCR) or transgenic plants expressing *AtYSL2* promoter::GUS fusions support a function for AtYSL2 in plant Fe and Zn homeostasis.

Results

Isolation of AtYSL2 from an Arabidopsis cDNA library

The open reading frame (ORF) of *AtYSL2* was amplified from an *Arabidopsis thaliana* Col-0 cDNA library and cloned into the pGEM[®]-T Easy vector for further subcloning.

Sequence analysis revealed that, in contrast to the database prediction (TAIR, <http://www.arabidopsis.org/>), the *AtYSL2* cDNA contained the additional exon sequences 1,011–1,028 bp and 1,488–1,505 bp (starting from ATG as position 1 in the genomic DNA; GenBank accession number AY648977) which were predicted to represent intron sequences. These additional exon sequences were also present in two cDNA sequences found in the database (accession nos AY139751 and BT005806).

A phylogenetic analysis of the *Arabidopsis* AtYSL homologs and ZmYS1 suggested that AtYSL proteins cluster into three subgroups, and one of them, containing AtYSL1, AtYSL2 and AtYSL3, is most closely related to ZmYS1 in terms of sequence (Fig. 1). Using the ClustalW software (Meg-

Align, DNASTAR, Madison, WI, USA), *AtYSL2* exhibited the closest homology to ZmYS1 with 59.8% identity at the amino acid level. The *AtYSL* homologs and *ZmYS1* encode proteins of approximately 73–80 kDa that possess typical membrane protein signatures of alternating transmembrane-spanning domains (TMDs) and hydrophilic loops. In general, a longer hydrophilic loop separates the first four TMDs from the following 8–10 TMDs (<http://www.cbs.dtu.dk/services/TMHMM-2.0>).

Expression of *AtYSL2* depends on the Fe and Zn nutritional status

To investigate whether *AtYSL2* might be involved in Fe homeostasis, gene expression dependence on the Fe nutritional status was studied by Northern analysis. Therefore, hydroponically grown Fe-sufficient *Arabidopsis* plants were transferred to Fe-deficient medium for 10 d (–Fe) and then resupplied for 24 h with 50 μ M Fe(III)-EDTA (–Fe+RS). As shown in Fig. 2A, *AtYSL2* expression could be detected in roots of Fe-sufficient and resupplied plants, but expression in roots was low under Fe starvation. In shoots, a weak expression could be detected only under Fe-sufficient conditions. In addition, we monitored the expression of *AtIRT1*, an Fe deficiency-induced gene encoding the major high-affinity Fe transporter in the *Arabidopsis* root epidermis (Vert et al. 2002). In agreement with data obtained by us and others (Connolly et al. 2002, Vert et al. 2003), *AtIRT1* expression was strongly enhanced under Fe-limiting conditions and repressed after Fe resupply (Fig. 2A, lower panel), which confirms that –Fe plants had been efficiently starved for Fe. Moreover, interveinal chlorosis in leaves of –Fe plants confirmed their Fe-deficient state. These data demonstrated that *AtYSL2* expression in roots and regulation is dependent on the Fe nutritional status in an opposite manner to *AtIRT1*, thus supporting a different role for *AtYSL2* in Fe homeostasis. In an independent approach, gene expression was

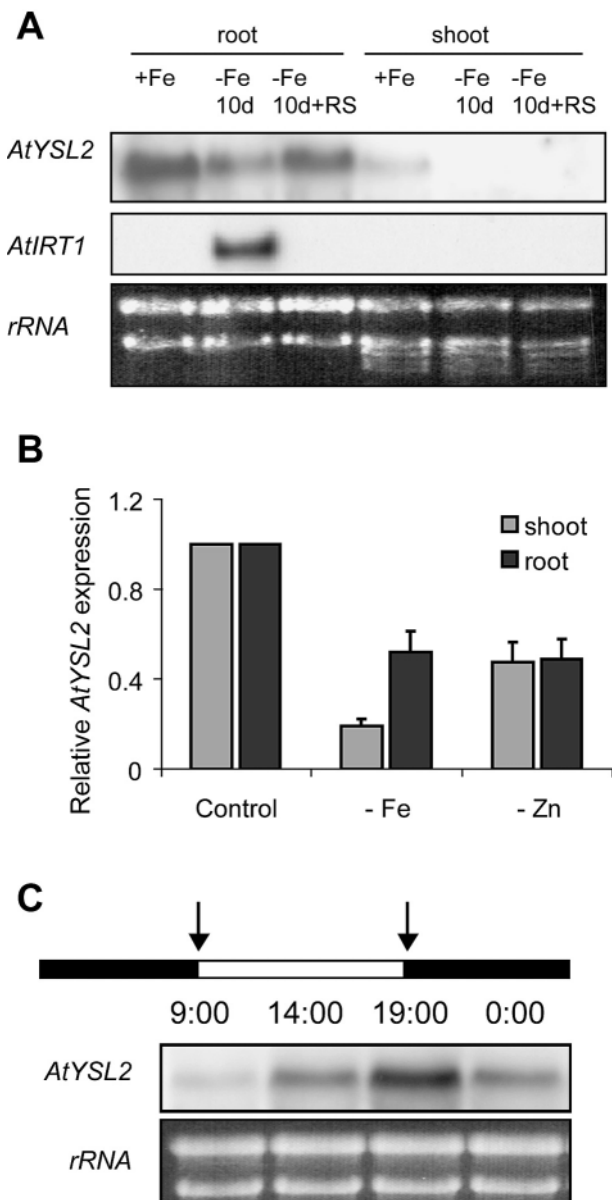


Fig. 2 (A) Gene expression of *AtYSL2* is dependent on the Fe nutritional status. RNA gel blot analysis was performed with hydroponically grown plants that were pre-cultured for 5 weeks in the presence of 50 μ M Fe(III)-EDTA and starved of Fe for 10 days (–Fe 10d) or starved of Fe for 10 d and then resupplied with 50 μ M Fe(III)-EDTA for 24 h (–Fe 10d+RS). Total RNA from shoots or roots was used for hybridization to the ORF of *AtYSL2* (upper panel) and *AtIRT1* (middle panel). As a loading control, the ethidium bromide staining of the nylon membrane is shown (lower panel). (B) Real-time PCR quantification of *AtYSL2* expression. Four-week-old wild-type plants were transferred for 5 d to Fe- or Zn-depleted media before harvesting. Detected amplicons were normalized to amplified products corresponding to *Arabidopsis tefA1*, *tefA2* and *tefA3* genes, encoding EF-1 α . (C) Diurnal regulation of *AtYSL2* gene expression. RNA gel blot analysis was performed with plants pre-cultured for 6 weeks under extended short day and Fe-sufficient conditions [onset of light 9 : 00 h, light to dark transition 19 : 00 h, 50 μ M Fe(III)-EDTA] and harvested at different time points. Total RNA from shoots or roots was used for hybridization to the complete ORF of *AtYSL2* (upper panel). As a loading control, the ethidium bromide staining of the nylon membrane is shown (lower panel).

investigated by real-time PCR. For this purpose, plants were grown during 5 d either in the presence of 100 μ M Fe(III)-EDTA or without Fe in the culture medium. The quantitative analyses revealed that Fe deficiency leads to a 2-fold decrease of the transcript levels in roots as compared with Fe-sufficient roots (Fig. 2B), confirming the Northern analysis. In addition, *AtYSL2* mRNAs accumulated four times less in shoots in conditions of Fe deficiency. The amount of transcript in shoots, however, was much lower than in roots (data not shown).

To assess the effect of Zn deficiency on *AtYSL2* expression, plants were grown in nutrient solution for 4 weeks and then transferred to Zn-deficient medium for 5 d. As for Fe, Zn starvation resulted in a 2-fold decrease in *AtYSL2* mRNA abundance, in both shoots and roots. The data obtained by Northern analysis and real-time PCR were in agreement with a third approach investigating the enzymatic activity of transgenic plants expressing an *AtYSL2* promoter:: β -glucuronidase (GUS) gene: for this purpose, transgenic plants were grown for 10 d under Fe- and Zn- sufficient conditions and then transferred to Zn- or Fe-depleted medium and analyzed for enzymatic GUS activity. GUS activity of Fe-deficient plants was reduced approximately 2-fold in roots and shoots (Fig. 3I). The effect was even more pronounced in Zn-deficient plants, where the enzymatic activity of the *AtYSL2* promoter-driven GUS gene was reduced by >10-fold in roots and >2-fold in leaves. The enzymatic GUS activity was consistent with the histochemical staining of transgenic plants, indicating a reduced GUS expression under Fe and Zn deficiency (Fig. 3C, D, respectively).

Expression of *AtYSL2* shows a diurnal rhythm

We then investigated whether *AtYSL2* expression depends on the diurnal rhythm. For this purpose, plants were grown under Fe-sufficient conditions and harvested at 9 : 00 h, 14 : 00 h, 19 : 00 h and 0 : 00 h. The expression level of *AtYSL2* in roots was highest at 19 : 00 h (at the end of the light period) and lowest at 9 : 00 h (at the end of the dark period, Fig. 2C). We therefore concluded that, similarly to *AtIRT1* and *AtFRO2*, expression of *AtYSL2* is subjected to diurnal regulation.

AtYSL2 is expressed in the root central cylinder

Root-specific expression of *AtYSL2* was confirmed further by promoter-reporter gene analysis. Twelve transgenic *Arabidopsis* lines, expressing an *AtYSL2* promoter::GUS fusion, were generated and examined with regard to tissue specificity of the *AtYSL2* promoter activity. GUS histochemical analyses were performed on plants selected in vitro for kanamycin resistance during 10 d and grown for another 5 d in the absence of kanamycin. In 10 out of 12 lines, the promoter was active in the central cylinder of the root (Fig. 3A). Three lines additionally showed a weak activity in leaves, which was restricted to the veins (Fig. 3B). In cross-sections of young roots, the promoter activity was localized in the pericycle as well as in the parenchyma of the central cylinder

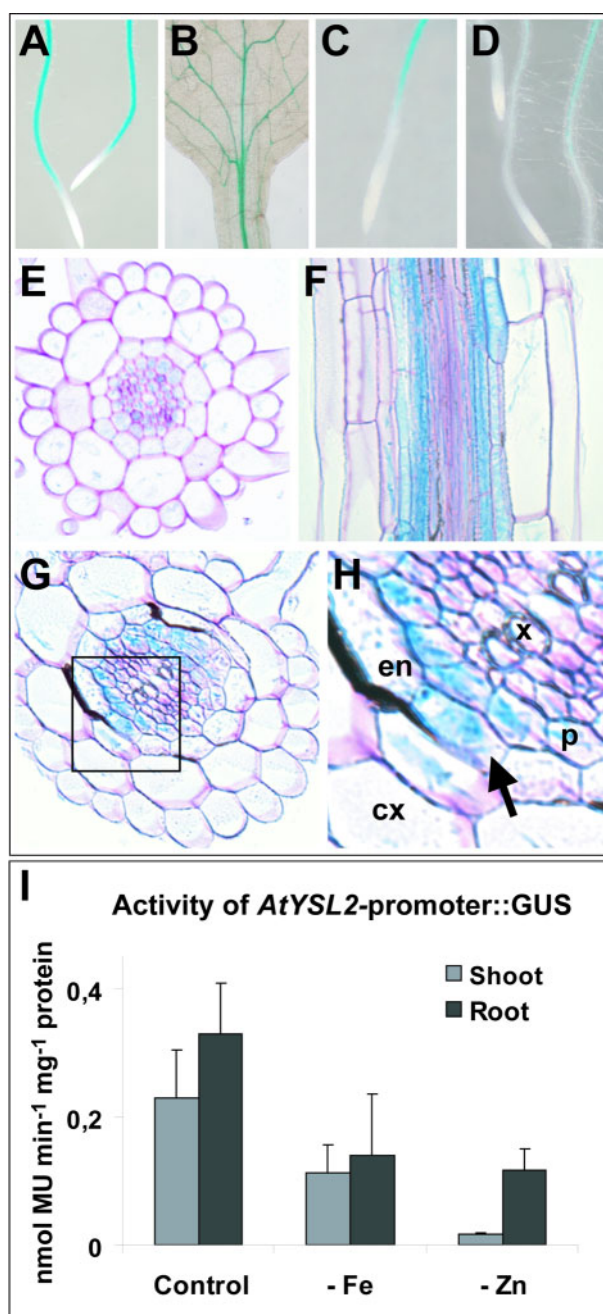
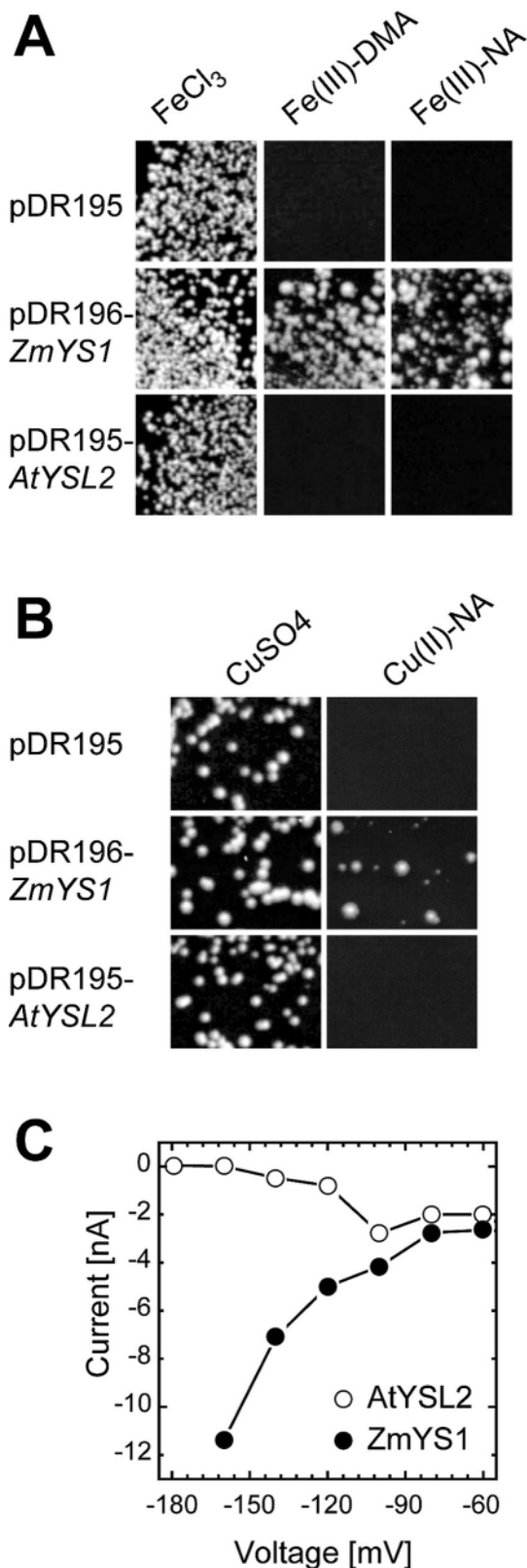


Fig. 3 (A–H) Analyses of *AtYSL2p*::GUS-expressing transgenic *Arabidopsis* plants by GUS histochemical staining. (A and B) Control nutrient condition: (A) young primary roots; (B) first leaf. (C and D) Roots of treated plants: (C) –Fe; (D) –Zn. (E–H) Sections of roots from transgenic plants grown in control conditions at different developmental stages: (E) cross-section of root hair zone; (F) mature roots; (G) secondary root-appearing zone; (H) insert in (G). cx, cortex; en, endodermis; p, pericycle; x, xylem. (I) β -Glucuronidase enzymatic activity measured in transgenic plants cultivated for 4 d on Fe- or Zn-deficient media.



(Fig. 3E). This pattern changed during root development, since mature roots also showed GUS staining in endodermal cells (Fig. 3F). In older parts of the root, the promoter remained active in the pericycle layer as well as in the endodermis, but only in those cells that faced the meta-xylem tubes (Fig. 3G, H).

Heterologous expression of AtYSL2 in yeast and Xenopus oocytes could not show a function in metal-chelate transport

ZmYSL1 has been shown to complement the growth defect of the *fet3 fet4* mutant, which is defective in high- and low-affinity Fe transport (Spizzo et al. 1997) on media containing Fe(III)-DMA (Curie et al. 2001) or Fe(II)-NA and Fe(III)-NA (Schaaf et al. 2004) as a sole Fe source. To investigate whether the selected *Arabidopsis* homolog was also able to complement the growth defect of the *fet3 fet4* mutant, *AtYSL2* was subcloned into the yeast expression vector pDR195 under control of the strong *PMA1* promoter fragment. Transformants were plated on media supplemented with different concentrations of Fe(II)-NA and Fe(III)-NA or the more easily available structural analog Fe(III)-DMA at different pH values. However, under any tested condition, growth of the yeast *fet3 fet4* mutant expressing *AtYSL2* was similar to that of yeast transformed with pDR195 alone (Fig. 4A). *AtYSL2* in pDR195 was further used for transformation of the Cu uptake-defective yeast mutant *ctr1*, which is unable to grow on media supplemented with low Cu and a non-fermentable carbon source (Dancis et al. 1994; Fig. 4B). In contrast to *ZmYSL1*, however, *AtYSL2* was not able to restore growth of *ctr1* on 6 μ M Cu(II)-NA.

AtYSL2 was then heterologously expressed in *Xenopus* oocytes and analyzed by two-electrode voltage clamp. For this purpose, oocytes injected with pOO2-*AtYSL2* or pOO2-*ZmYSL1* cRNA were clamped at -70 mV in choline-based buffer solution at pH 6.0 and then superfused with buffer containing different metal-NA chelates. As expected, in control oocytes injected with cRNA encoding *ZmYSL1*, currents were induced

Fig. 4 (A) Heterologous expression of *AtYSL2* and *ZmYSL1* in the yeast *fet3 fet4* mutant. Yeast cells were streaked on media supplemented with 1.3 μ M Fe(III)-DMA, pH 6.0 (DMA in 10-fold excess) or 20 μ M Fe(II)-NA, pH 7.5 (NA in 1.2-fold excess); control plates were supplemented with 30 μ M FeCl₃. Similar results were obtained on media supplemented with 1.3 μ M Fe(III)-DMA at pH 5.0, pH 7.0 and pH 8.0 (DMA in 10-fold excess), with 20 μ M Fe(III)-DMA at pH 7.5 (DMA in 2.5-fold excess), with Fe(II)-NA at 7.5 and 20 μ M, and with Fe(III)-NA at 50 and 100 μ M (NA in 1.2-fold excess at pH 7.5) (data not shown). (B) Transformants of the *ctr1* yeast mutant were streaked on media supplemented with 3% glycerol as a sole carbon source, the appropriate supplements and either 20 μ M CuSO₄ (control) or 6 μ M Cu(II)-NA, pH 7.5 (NA in 2-fold excess). (C) Two-electrode voltage clamp analysis of *AtYSL2* in *Xenopus* oocytes. Voltage dependence of currents induced by 24 μ M Fe(III)-NA (pH 7.5) in oocytes injected with *AtYSL2* cRNA (open circles). As a control for the formation of the Fe(III)-NA complex, currents induced by Fe(III)-NA in oocytes injected with *ZmYSL1* cRNA were recorded (filled circles).

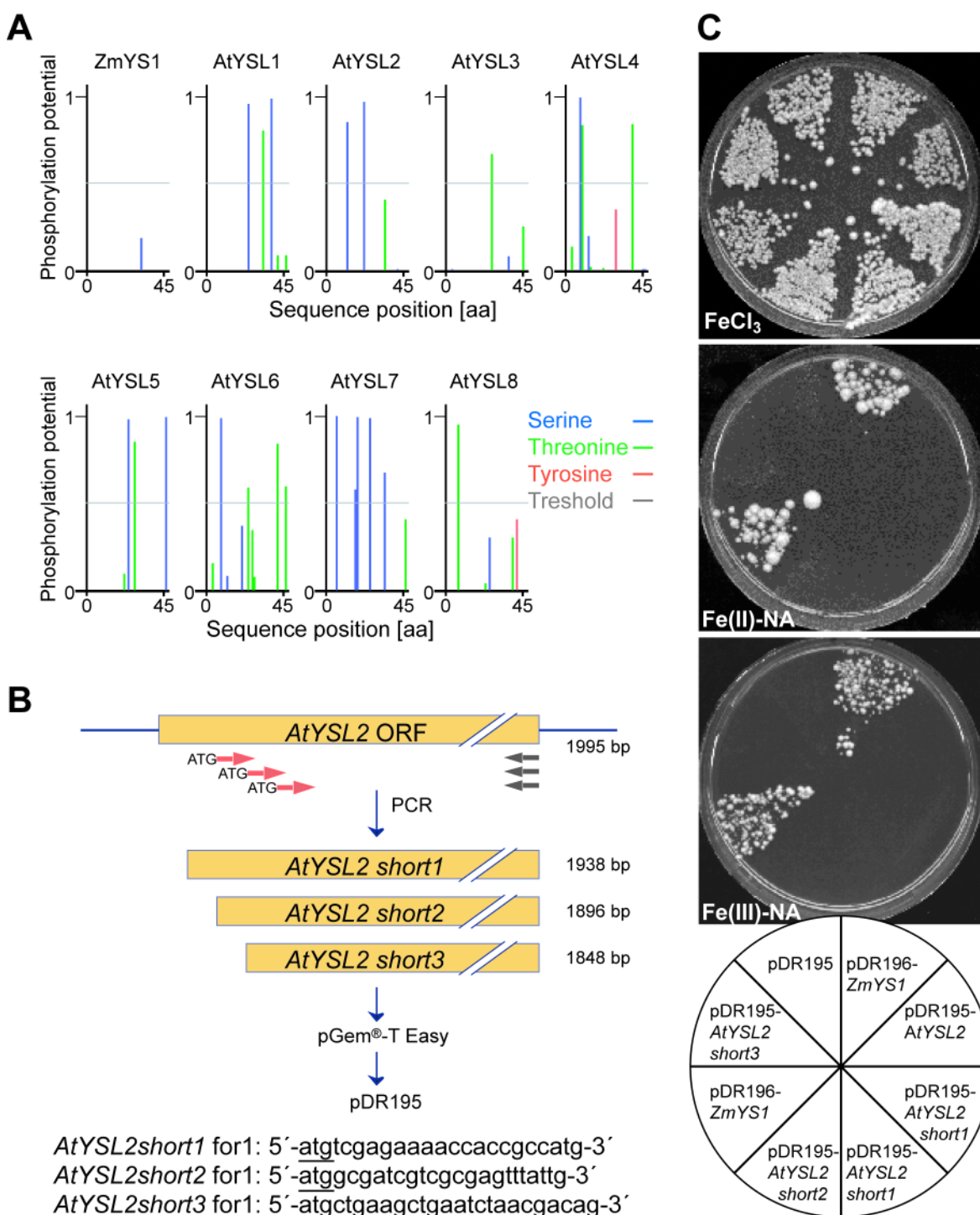


Fig. 5 (A) Prediction of phosphorylation sites in the N-terminal region of ZmYS1 and the AtYSL homologs. Phosphorylation sites in the 45 N-terminal amino acids of the transporters were predicted by the NetPhos 2.0 program (www.cbs.dtu.dk/services/NetPhos) (B) Construction of the N-terminal truncated versions of AtYSL2. Primers were designed to hybridize to *AtYSL2* at positions 61 bp (*AtYSL2short1* for1), 103 bp (*AtYSL2short2* for1) and 151 bp (*AtYSL2short3* for1) relative to position 1 from the initial ATG. Each forward primer contained an additional ATG at the 5' end (underlined) to allow translation of the truncated AtYSL2 version at this position. (C) Expression of N-terminal truncated versions of AtYSL2 in yeast. Growth of the yeast *fet3 fet4* mutant (DEY1453) transformed with pDR196-ZmYS1, pDR195-*AtYSL2*, pDR195-*AtYSL2short1*, pDR195-*AtYSL2short2*, pDR195-*AtYSL2short3* or empty pDR195 on media supplemented with 50 μ M Fe(II)-NA (left), 35 μ M Fe(III)-NA (right) or 30 μ M FeCl₃. Similar results were obtained when plating transformants on media supplemented with 7.5 μ M Fe(II)-NA or 7.5 μ M Fe(III)-NA at pH 7.5 (data not shown). No growth differences could be observed at 10 μ M FeCl₃ (data not shown). Plates were incubated at 30°C for 10 d (Fe-NA) or 5 d (FeCl₃).

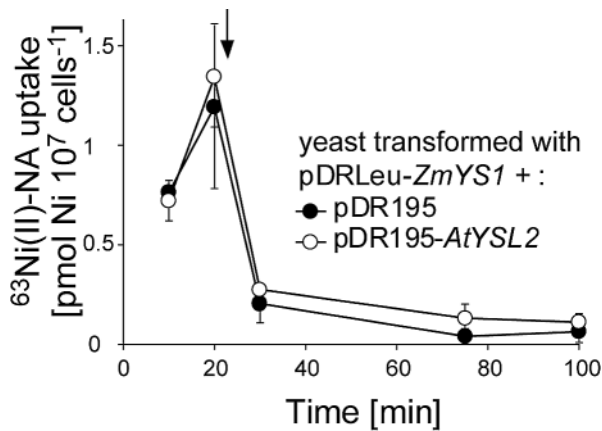


Fig. 6 Uptake and release of Ni(II)-NA in AtYSL2-expressing yeast. Yeast cells were co-transformed with pDR196-*ZmYS1* and pDR195-*AtYSL2* (open circles) or empty pDR195 (filled circles). Midlog phase cells of transformed BY4741, concentrated to OD12, were pre-incubated for 15 min at 30°C before uptake was started by addition of $^{63}\text{Ni(II)-NA}$ solution (pH 6.5) to obtain a final concentration of 3.5 μM . After 20 min uptake (arrow), cells were resuspended in release buffer (3% glucose, 20 mM NaH_2PO_4 , 10 mM EDTA and 50 mM citric acid, pH 4) and incubated further at 30°C.

by 24 μM Fe(III)-NA (Fig. 4C), 50 μM Fe(II)-NA or 50 μM Ni(II)-NA (data not shown). Observed currents corresponded to the net influx of positive charge (Schaaf et al. 2004). However, neither 24 μM Fe(III)-NA (Fig. 4C) nor any of the other metal-NA chelates induced currents in oocytes injected with cRNA of *AtYSL2*, which behaved like water- or non-injected control oocytes (data not shown).

Predicted N-terminal phosphorylation sites suggested post-translational regulation of *AtYSL2* and other *AtYSL* homologs

Since the activity of transport proteins might depend on the phosphorylation status of regulatory N-terminal domains, the N-termini of AtYSL proteins were analyzed for possible phosphorylation sites employing the NetPhos 2.0 programme (www.cbs.dtu.dk/services/NetPhos). As shown in Fig. 5A, all *Arabidopsis* homologs contain at least one (*AtYSL3* and *AtYSL8*) or several (*AtYSL1*, *AtYSL2*, *AtYSL4*, *AtYSL5*, *AtYSL6* and *AtYSL7*) putative phosphorylation sites in the N-terminal 45 amino acids, whereas *ZmYS1* was not predicted to possess phosphorylation sites in this region. Thus, N-terminal autoinhibition of *AtYSL2* might be responsible for its lack of functionality. N-terminally truncated versions of several transporters lacking these phosphorylation sites, such as the *Arabidopsis* vacuolar $\text{Ca}^{2+}/\text{H}^+$ antiporter *AtCAX1* (Pittman and Hirschi 2001, Pittman et al. 2002) and the vacuolar $\text{Mn}^{2+}/\text{H}^+$ antiporter *AtCAX2* (Schaaf et al. 2002), showed activity in contrast to the corresponding full-length versions. Therefore, a PCR-based approach was set up to generate N-terminally truncated versions of *AtYSL2* as illustrated in Fig. 5B. However, none of these versions was able to complement the growth

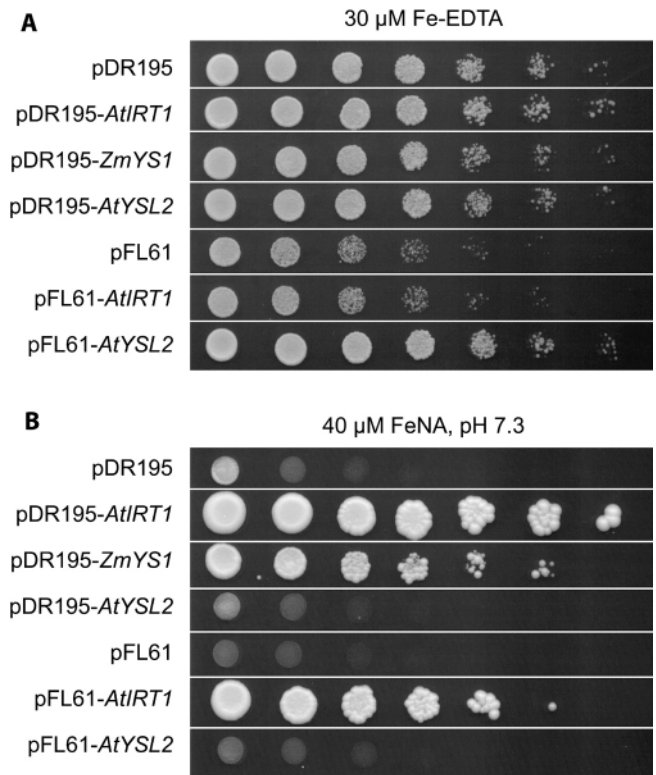


Fig. 7 Growth complementation of the Fe uptake-defective yeast strain *fet3 fet4* is dependent on vector type and form of the Fe supply. *fet3 fet4* was transformed with either empty pDR195 or pDR195 harboring the cDNAs of *AtIRT1*, *ZmYS1* or *AtYSL2*, and alternatively with empty pFL61 or pFL61 harboring the cDNAs of *AtIRT1* or *AtYSL2*. Yeast transformants were grown in liquid YNB medium for 48 h. A 1 ml aliquot of liquid culture was washed in 10 \times TE, pH 6.5, and resuspended in water to a final OD of 4. A 10 μl aliquot of a series of 5-fold dilutions was spotted onto plates containing either (A) 30 μM Fe(III)-EDTA or (B) 40 μM Fe(III)-NA adjusted to pH 7.4 by MES/TRIS. Plates were incubated at 30°C for 2 d (A) or 4 d (B).

defect of the yeast *fet3 fet4* strain on media supplemented with 50 μM Fe(II)-NA or 35 μM Fe(III)-NA (Fig. 5C) and other Fe(II)-NA and Fe(III)-NA concentrations or on low concentrations of FeCl_3 (data not shown).

Co-expression of *ZmYS1* with *AtYSL2* did not affect growth on Fe-NA or alter uptake and release of Ni-NA in yeast

Since failure of *AtYSL2* to complement the growth defect of the yeast *fet3 fet4* mutant or to mediate metal-NA-induced currents in oocytes might be due to a function of *AtYSL2* in metal-NA release rather than in metal-NA uptake, an experiment was set up that took into account a potential function of *AtYSL2* in substrate export. For this purpose, *ZmYS1* was co-expressed with pDR195-*Leu-ZmYS1* and pDR195-*AtYSL2*. This approach attempted to load yeast cells with Ni(II)-NA via *ZmYS1* to analyze subsequently a potential *AtYSL2*-mediated release of Ni(II)-NA. In this experiment, NA-chelated Ni was employed, since we observed in previous studies less precipita-

tion and adsorption of the metal to the matrix (e.g. yeast cell walls) when compared with Fe(II)-NA, thus allowing detection of small quantities more reliably (Schaaf et al. 2004 and unpublished results). As a control, yeast cells co-transformed with pDR195*Leu-ZmYS1* and the empty vector pDR195 were used. After a 20 min incubation period in Ni(II)-NA, yeast cells were washed and transferred to release buffer. As shown in Fig. 6, no statistically significant differences in uptake or release rates between *AtYSL2*-expressing cells and control cells were found. This experiment was also designed to investigate a potential intracellular localization of *AtYSL2*: if this homolog mediated transport of Ni(II)-NA into internal compartments, one might expect that the release of ⁶³Ni would be decreased or held up after *ZmYS1*-mediated loading.

The yeast expression vectors pDR195 and pFL61 affect yeast growth differently

In the study of DiDonato et al. (2004), which was published while this manuscript was being reviewed, a growth complementation of Fe and Cu uptake-defective yeast mutants by *AtYSL2* on Fe(II)- or Cu(II)-NA was shown, which contrasted with our own observations (Fig. 4). We therefore tested whether this discrepancy with our experiments might be related to the use of different yeast expression vectors and transformed the *fet3 fet4* yeast mutant with *AtYSL2* either in pDR195 or in pFL61 as used by DiDonato et al. (2004). A direct comparison of yeast growth under non-limiting Fe supply (30 μ M Fe-EDTA) showed that yeast colonies were smaller when transformed with empty pFL61 relative to empty pDR195 (Fig. 7A). Impaired growth was not due to Fe deficiency because increasing Fe concentrations did not reverse the growth differences between pFL61 and pDR195 transformants (data not shown) and because pFL61-*AtIRT1* transformants did not show better growth relative to cells transformed with pFL61 alone (Fig. 7A). Colony development of *AtYSL2*-transformed cells, however, was only superior to that of the transformants with empty vector when the pFL61 vector was used but not when pDR195 was used. Moreover, growth of pFL61-*AtYSL2* transformants exactly matched that of pDR195 transformants irrespective of whether they carried a cDNA of *AtIRT1*, *ZmYS1* or *AtYSL2*. The relative growth advantage suggested by the comparison of pFL61-*AtYSL2* transformants with empty vector transformants clearly agreed with the data published by DiDonato et al. (2004). However, the apparent *AtYSL2*-mediated growth advantage was not related to Fe or the presence of Fe(II)-NA, because it appeared under non-limiting Fe supply and in the absence of NA (Fig. 7A). In contrast, under supply of 40 μ M Fe(II)-NA, *AtYSL2* could not improve yeast growth, while expression of *ZmYS1* or *AtIRT1* clearly overcame Fe-limited growth depression (Fig. 7B). Also under these conditions, pFL61-transformed cells tended to grow poorly compared with pDR195-transformed cells.

Discussion

In non-graminaceous plants such as *Arabidopsis*, the transport of chelated transition metals across the plasma membrane or across intracellular membranes might provide a transport pathway that prevents the cytoplasm from deleterious effects mediated by free metals along the Fenton reaction. Recent studies in the hyperaccumulating plant *Thlaspi caerulescens* provide in addition increasing evidence for the formation of Ni-NA complexes under high Ni supply and transport of Ni-NA in the xylem, most probably for detoxification purposes (Vacchina et al. 2003). Based on the findings that NA is involved in inter- or intracellular trafficking of Fe and other metals (Pich et al. 2001, Takahashi et al. 2003), and that a member of the YS1/YSL transporter family, *ZmYS1*, also transports NA-chelated metals (Schaaf et al. 2004), we addressed the question of whether *AtYSL2*, one of the closest *Arabidopsis* homologs to *ZmYS1* (Fig. 1), acts as a metal-NA transporter.

Heterologous expression suggests a different function for AtYSL2 and ZmYS1

Neither growth complementation of the yeast mutants *fet3 fet4* and *ctr1* nor two-electrode voltage clamp analysis allowed the demonstration of the functionality of *AtYSL2*, although in both assays the positive control, *ZmYS1*, mediated metal-chelate transport (Fig. 4). A simple explanation for the failure to show the functionality could be that the correct substrate has not yet been found. Indeed, in several cases, sequence homology between transporters did not allow us to come to a conclusion as to the identity of transported substrates. For instance, the OPT family, which includes *ZmYS1* and the *AtYSL* homologs, additionally includes members mediating the transport of tetrapeptides such as the *Schizosaccharomyces pombe* OPT member ISP4 (Lubkowitz et al. 1998) or of the tripeptide glutathione such as SchGHT1 (Bourbouloux et al. 2000). In future experiments, it may thus be essential to conduct a large-scale screening of possible substrates for *AtYSL2*. The versatile oocyte expression system, which allowed the setting up of an expanded list of substrates transported by *ZmYS1*, is certainly a suitable approach for this purpose (Schaaf et al. 2004).

An intracellular localization of *AtYSL2* might also hamper the functional characterization of transporters in heterologous systems and could explain the failure of yeast complementation and functional analysis in *Xenopus* oocytes in our study. Localization in yeast is in many cases similar to the endogenous localization, as shown for the *Arabidopsis* vacuolar pyrophosphatase and the vacuolar ATP-binding cassette transporter *AtMRP2* (Kim et al. 1994, Liu et al. 2001) or as evidenced for the mitochondrial basic amino acid carriers *AtmBAC1* and *AtmBAC2* (Catoni et al. 2003, Hoyos et al. 2003). However, localization in the plasma membrane in the endogenous system is not in all cases a prerequisite for complementation of yeast mutants defective in nutrient uptake, as shown for *AtNRAMP3* which complemented the *fet3 fet4* yeast

mutant (Thomine et al. 2000), but for which green fluorescent protein (GFP) fusions localized to tonoplast when expressed in *Arabidopsis* protoplasts (Thomine et al. 2003). Therefore, cauliflower mosaic virus 35S-driven AtYSL2–GFP fusion proteins were transiently expressed in *Arabidopsis* protoplasts and analyzed by confocal microscopy. Although in several protoplasts GFP-dependent fluorescence localized to internal compartments (data not shown), fluorescence was too weak to draw firm conclusions. Other methods should therefore describe the native subcellular localization of AtYSL2.

Autoinhibitory domains have been reported to cause post-transcriptional down-regulation of protein activity in various animal, yeast and plant transporters (Pittman and Hirschi 2001). For transporters in intracellular membranes, these domains were mainly localized at the N-terminus, and N-terminal truncation could restore the activity of these proteins as shown for the endoplasmic reticulum-localized Ca^{2+} -ATPase ACA2 (Harper et al. 1998), the tonoplast Ca^{2+} -ATPases ACA4 (Geisler et al. 2000) and BCA (Malmström et al. 2000), the tonoplast $\text{Ca}^{2+}/\text{H}^{+}$ exchanger AtCAX1 (Pittman and Hirschi 2001) and the tonoplast $\text{Mn}^{2+}/\text{H}^{+}$ exchanger AtCAX2 (Schaaf et al. 2002). N-terminal inhibition has also been shown for the plasma membrane-localized Ca^{2+} -ATPase SCA1 (Chung et al. 2000). In the case of AtCAX1 and ACA2, the inhibitory effect of these domains depended on the phosphorylation status of serine residues at position 25 and 45, respectively (Hwang et al. 2000, Pittman and Hirschi 2001). Analysis of the encoded AtYSL proteins revealed that in contrast to ZmYS1, all AtYSL2 homologs contained one or several predicted phosphorylation sites within the first 45 amino acids (Fig. 5A). Therefore, truncated versions of AtYSL2 were generated and tested for functionality. However, none of the truncated versions could complement growth of the yeast *fet3 fet4* mutant (Fig. 5C). In addition, Ni–NA transport was not affected when N-terminal truncated versions of AtYSL2 were co-expressed with ZmYS1 (data not shown).

The AtYSL2-mediated advantage for yeast growth depended on the yeast expression vector and not on the supply of Fe(II)–NA as an Fe source

In the study of DiDonato et al. (2004), the proof of AtYSL2 functionality as an Fe(II)–NA transporter was based exclusively on a yeast complementation study. A growth comparison between pFL61- and pFL61-*AtYSL2*-transformed yeast cells on 4 μM Fe in the presence of 5 μM NA yielded better growth of Fe uptake-defective yeast cells, and similarly, yielded better growth of Cu uptake-defective cells when Cu was supplied in the presence of NA (DiDonato et al. 2004). We could reproduce this apparent difference in growth complementation; however, we clearly observed that it occurred independently of the Fe supply and in the absence of NA. Under non-limiting Fe supply of 30 μM Fe-EDTA, pFL61-transformed yeast cells clearly grew more slowly than pDR195 transformants, indicating that the empty pFL61 vector alone con-

fers a relative growth depression (Fig. 7A). Irrespective of the employed vector system, however, AtYSL2 could not complement yeast growth when Fe(II)–NA was supplied at 40 μM (Fig. 7B). We cannot yet explain the reason for the AtYSL2-mediated growth difference in the pFL61 vector system and why it is restricted to pFL61. It is clear, however, that the AtYSL2-mediated growth difference under these conditions did not depend on Fe limitation and on the supply of Fe–NA as an Fe source. We therefore conclude that the yeast complementation assay employed by DiDonato et al. (2004) does not allow identification of AtYSL2 as an Fe–NA transporter. In future, it will thus be important to verify yeast complementation approaches by metal–chelate uptake or electrophysiological studies in heterologous systems or in transgenic plants.

Transcriptional regulation of AtYSL2 supports a role in Fe and Zn homeostasis

As shown by three independent approaches, Northern analysis, real-time PCR and promoter–reporter gene analysis, *AtYSL2* is expressed mainly in roots, repressed under Fe and Zn starvation and upregulated upon Fe resupply (Fig. 2A, B, Fig. 3). A decreased expression under Fe starvation clearly argues in favor of a role for AtYSL2 in Fe storage or Fe detoxification rather than in Fe uptake or acquisition as postulated for ZmYS1 (von Wirén et al. 1994). The transcriptional regulation of *AtYSL2* resembled that of the NAS genes *OsNAS3* and *ZmNAS3*, for which expression was decreased under Fe deficiency (Inoue et al. 2003, Mizuno et al. 2003). Moreover, *AtYSL2* is additionally regulated by Zn. Expression of *AtYSL2* was repressed in Zn-deficient plants, supporting the view that Fe and Zn share common pathways in chelation as well as in membrane transport. Several plant Fe transporters with Zn transport capabilities have been described, including AtIRT1, AtIRT2, AtNRAMP3 and ZmYS1 (Eide et al. 1996, Vert et al. 2001, Vert et al. 2002, Thomine et al. 2003, Schaaf et al. 2004). It is noteworthy that both Fe and Zn participate in regulating the Fe uptake machinery in *Arabidopsis* since accumulation of *IRT1* and *FRO2* transcripts upon Fe deficiency is repressed by Zn supply (Connolly et al. 2003). However, the Zn control seems to be exerted at the post-transcriptional level for *IRT1* and *FRO2* genes, while Fe deficiency and Zn deficiency most probably regulate *AtYSL2* expression transcriptionally as indicated by the GUS expression analyses.

The diurnal regulation of *AtYSL2* was reminiscent of the expression pattern of *AtIRT1* and *AtFRO2*, which showed an increase of transcript levels during the light period (Vert et al. 2003). For *AtIRT1* and *AtFRO2*, this regulation does not seem to be controlled by an endogenous circadian rhythm rather than directly or indirectly by light (Vert et al. 2003). A diurnal rhythm in the transcriptional regulation of plant membrane transporters has also been described for nitrate, ammonium and sulfate transporters (Gazzarrini et al. 1999, Lejay et al. 1999, Lejay et al. 2003). A more detailed study revealed that substrate transport and expression of these transporters was

enhanced by an increase in light intensity and by external sugar supply, indicating that this regulation depends on the stimulation by photoassimilates (Lejay et al. 2003). These authors further postulated that the induction of the nitrate transporter gene *AtNRT2;1* during the light period depended on the glycolysis pathway or a metabolite downstream of the reaction catalyzed by hexokinase. Nutrient acquisition is a process that requires free energy. Stimulation of nutrient transporters by light may reflect an adaptation to the huge energy demand of nutrient transport processes and the subsequent metabolic pathways. This seems also to apply for AtYSL2 and thus supports its putative function in Fe and Zn transport.

Promoter–GUS analysis reveals vascular localization of AtYSL2

Analyses of transgenic plants expressing the GUS gene under control of a 1.12 kb *AtYSL2* promoter fragment confined expression of *AtYSL2* to the vascular tissue (Fig. 3). The localization of *AtYSL2* promoter-driven GUS expression in pericycle and endodermis cells facing the meta-xylem tubes resembled the expression pattern of the outwardly rectifying K⁺ channel SKOR (Gaymard et al. 1998), the boron transporter AtBOR1 (Takano et al. 2002) or the phosphate transporter AtPHO1 (Hamburger et al. 2002), which are all involved in xylem loading. The article by DiDonato et al., which was published during the review process of the present study, proposes a function for AtYSL2 in the transport of NA-chelated metals for the lateral movement of NA-chelated metals in the vasculature. This conclusion is based on the localization of AtYSL2–promoter–GUS in the vasculature and the subcellular localization of stably transformed AtYSL2–GFP in lateral plasma membranes of elongated cells within the vascular tissue. While our AtYSL2–promoter–GUS studies are fully in agreement with the high promoter activity in the vasculature, transient expression of AtYSL2–GFP in *Arabidopsis* protoplasts did not allow characterization of the subcellular localization (unpublished data), perhaps due to a loss of cell polarity and disturbed AtYSL2 targeting in suspension cultures. Despite its localization in the plasma membrane, however, it remains unclear whether AtYSL2 is indeed involved in xylem loading. If so, AtYSL2 might function as an Fe–chelate exporter even though our co-expression tests with ZmYS1 in yeast cells might argue against such a possibility (Fig. 6).

While the transcriptional regulation and the *AtYSL2* promoter–reporter gene analyses support a function for AtYSL2 in Fe homeostasis, a function for this Fe(III)–PS transporter homolog could not be established in the present study. Since most of the functional assays were conducted in parallel with ZmYS1, which reliably showed functionality in the same approach, we conclude that a different transport mechanism or substrate specificity applies for the in planta function of AtYSL2. However, it is also possible that *AtYSL2* is not targeted to the plasma membrane in heterologous expression systems. To elucidate this function in future approaches, the

analysis of *AtYSL2*-overexpressing plants and *AtYSL2* T-DNA insertion lines is encouraged.

Materials and Methods

Plasmids, yeast strains and growth conditions

DNA manipulations were carried out using standard protocols (Sambrook et al. 1989). Yeast media, were prepared using standard recipes (Rose et al. 1990). The ORF of *AtYSL2* was amplified by PCR from an *A. thaliana* Col-0 cDNA library (kindly provided by Karin Schumacher, ZMBP, Tübingen, Germany) using the primers 5'-ATGG-AAAACGAAAGGGTTGAG-3' and 5'-TTAATGAGCCGAGTGA-AGTTC-3'. PCR products were A-tailed, cloned into the pGEM[®]-T Easy Vector (Promega, Madison, WI, USA) following the manufacturer's instructions, sequenced and submitted to GenBank under accession number AY648977.

The *AtYSL2* ORF was subcloned into the yeast expression vector pDR195 (Rentsch et al. 1995) using the *NotI* restriction sites. *AtYSL2* was subcloned from the pGEM[®]-T Easy vector into the oocyte expression vector pOO2 (Ludewig et al. 2002) using the *Apal*–*PstI* restriction sites. The construction of pOO2–*ZmYS1* was described previously (Schaaf et al. 2004). The construct pDR195–*Leu-ZmYS1* was generated by subcloning *ZmYS1* from pDR196–*ZmYS1* (Schaaf et al. 2004) into pDR195–*Leu* at the *Bam*HI restriction sites. The pDR195–*Leu* vector is a derivative of the yeast expression vector YEplac181, in which a 1.1 kb *Hind*III–*Sph*I fragment of pDR195 was inserted using *Hind*III–*Sph*I (Kattie Luyten; Sympore GmbH, Tübingen, Germany, personal communication). Yeast transformed with the resulting vector pDR195–*Leu* and its derivatives can be selected on leucine-free medium. The short N-terminal truncated versions of *AtYSL2* were cloned into the pGEM[®]-T Easy vector and subcloned into pDR195 as illustrated in Fig. 5. The pFL61/AtYSL2 construct kindly provided by Dr. Elsbeth Walker was published earlier in DiDonato et al. (2004).

Yeast strains used for heterologous expression were the *ctr1* mutant (BY4741; Mat a; his3Δ1; leu2Δ0; met15Δ0; ura3Δ0; YPR124w::kanMX4, accession No. Y05539 from Euroscarf), its isogenic wild type (BY4741, Mat a; his3Δ1; leu2Δ0; met15Δ0; ura3Δ0; Euroscarf accession No. Y00000) and the *fet3 fet4* mutant (DEY1453, MATα/MATα ade2⁺/can1/can1 his3/his3 leu2/trp1/trp1 ura3/ura3 fet3-2:HIS3/fet3-2:HIS3/fet4-1:LEU2/fet4-1:LEU2, Spizzo et al. 1997). Yeast cells were transformed by the LiAc method (Gietz et al. 1992) and transformants were selected on uracil-deficient or uracil- and leucine-deficient medium containing 1% arginine as nitrogen source and the appropriate supplements.

To support growth of the *fet3 fet4* mutant, solid YNB medium contained additionally 30 μM FeCl₃, while the liquid YPD medium was acidified to pH 5.0 with HCl.

For growth tests, a single colony was washed in 1 ml of 10× TE (pH 7.5) and resuspended in sterile water to obtain an OD (600 nm) of 0.09. Cells were streaked on uracil-deficient or uracil- and leucine-deficient YNB medium, containing 0.1% arginine, 3% glucose, 0.01% tryptophan, histidine and methionine (and leucine when appropriate), and the respective Fe or Cu source. For selective growth of *ctr1* transformants, glucose was substituted by 3% of the non-fermentable carbon source glycerol.

Uptake experiments in yeast were performed as described in Schaaf et al. (2004). In a release experiment, yeast cells were incubated for 20 min in uptake solution, washed in release buffer, consisting of 3% glucose, 20 mM NaH₂PO₄, 10 mM EDTA and 50 mM citric acid adjusted to pH 4 with NaOH, and resuspended in release buffer to obtain an OD (600 nm) of 0.6. The release solution was incubated further at 30°C while shaking at 500 rpm. A 100 μl aliquot of uptake solu-

tion or 1 ml of release solution were diluted in 10 ml of 10 mM EDTA (pH 5.0, adjusted with NaOH) and filtered (glass microfiber filters, GF/C, Whatman, Maidstone, UK) using a vacuum filtration assembly (Hofer Pharmacia Biotech Inc., San Francisco, CA, USA). Filter membranes were analyzed by addition of 3 ml of 1% HCl and 3 ml of scintillation cocktail (Quicksafe A, Zinsser Analytic, Frankfurt, Germany) and liquid scintillation counting.

Plant cultivation and Northern analysis

Arabidopsis thaliana Col-0 was grown in hydroponic culture under short day conditions at 50% relative humidity with a light intensity of $150 \mu\text{E s}^{-1} \text{m}^{-2}$ and a day/night temperature regime of 10 h (9 : 00–19 : 00) at 22°C and 14 h at 19°C, respectively. For this purpose, 1.5 ml Eppendorf tubes (Hamburg, Germany) were cut at the 1 ml sign and sealed with a nylon net (\varnothing 400 μm) by heating the Eppendorf cups at the bottom. The lids of the tubes were removed and the Eppendorf cups were filled with quartz sand (\varnothing 0.6–1.2 mm) that had been washed three times in deionized water and dry sterilized. About 30 of these cups were placed in a perforated insulating mat floating on nutrient solution in 2.5 liters pots and 5–10 seeds were placed on top of one sand-filled Eppendorf tube. In the first week, pots contained 20 mg l^{-1} CaSO_4 in deionized water and transparent plastic panes covered the seeds. From the second week on, this solution was replaced by nutrient solution consisting of 1.8 mM KNO_3 , 1 mM CaSO_4 , 1 mM MgSO_4 , 0.5 mM KH_2PO_4 , 0.22 mM $(\text{NH}_4)_2\text{SO}_4$, 50 μM Na-Fe(III)-EDTA unless indicated otherwise, 25 μM H_3BO_3 , 2.5 μM MnCl_2 , 0.25 μM ZnSO_4 , 0.25 μM CuSO_4 and 0.25 μM $\text{NH}_4\text{Mo}_7\text{O}_{24}$. After 3 weeks, the nutrient solution was aerated and, from the fourth week onwards, the nutrient solution was changed every 3 d. After 4 weeks, the Eppendorf tubes containing the seedlings were transferred to stable PVC trays, staying on top of the 2.5 liters pots to dry out the sand, thereby reducing algal growth. The nutrient solution did not touch the rim of the Eppendorf tubes, but roots remained almost completely immersed in the nutrient solution. Plants were harvested after 7 weeks.

For Northern analysis, 20 μg of total root or shoot RNA were separated by gel electrophoresis and transferred to a Hybond-N⁺ membrane (Amersham Biosciences Europe GmbH, Freiburg, Germany) following standard protocols. For *AtIRT1* and *AtYSL2*, fragments obtained by *NotI* restriction digests of pFL61-*IRT1* and pDR195-*AtYSL2*, respectively, were used as a probe.

Real-time PCR

Total RNA was extracted from plants grown for 4 weeks in control hydroponic culture and transferred for another 5 d to Fe- or Zn-free media before collection of samples. A 5 μg aliquot of total RNA, treated with RQ1 RNase-free DNase (Promega, Madison, WI, USA) for 2 h at 37°C, was used as template for synthesis of the first strand of DNA. A total of 100 U of M-MLV reverse transcriptase (Promega, Madison, WI, USA) and 10 pmol of poly(dT) were used to initiate the reaction (in 20 μl volume). The resulting single-stranded DNA was diluted 5 \times in TE buffer (0.5 M Tris-HCl pH 8; 0.5 M EDTA); 0.2 μl of this mix was used as template for further PCRs. The real-time PCR was performed using the Light Cycler system (Roche, Penzberg, Germany) with the 'LC Fast Start DNA Master SYBR Green I' kit (Roche, Penzberg, Germany). Reactions were run for 50 cycles as follows: 3 s at 95°C, 7 s at 54°C, 4 s at 72°C using the *AtYSL2*-3'-untranslated region-specific primers (5'-GGCAGAAAGATTTTCCAGAC-3' and 5'-TCCCTCTTAACTGTCTACTCC-3'). Normalization of the values was based on the amount of *EF-1 α* single-stranded DNA (5'-GTCGATTCTGGAAAGTCGACC-3' and 5'-AATGTCAATGGT-GATACCACGC-3').

Generation of transgenic plants

GUS analyses were performed on 12 transgenic *Arabidopsis* T2 lines expressing a promoter *AtYSL2-uidA* fusion. A 1.12 kb fragment of the *AtYSL2* genomic sequence located upstream of the *ATG* was amplified by PCR using the primers 5'-CCCAAGCTTAGAAAAGT-GGAATGGTCTATAC-3' and 5'-CGGCCATGGGAAGAAAACGAA-TCTC-3', thereby introducing a *HindIII* site in 5' and a *NcoI* site in 3'. The *HindIII*-*NcoI* PCR fragment was cloned in translational fusion with the *uidA* gene in the pBKS-GUS vector (Eyal et al. 1995). The *HindIII*-*XbaI* fragment of the resulting plasmid, containing the *AtYSL2* promoter fused to the *uidA* gene, was subsequently inserted into the pBIN19 vector at the respective restriction sites. *Arabidopsis* Col-0 plants were transformed via *Agrobacterium*-mediated transformation (strain MP90) using the floral dip method (Clough and Bent 1998) and transformed plants were selected on kanamycin.

GUS expression analyses

Histochemical GUS analysis. Transgenic plants were grown in vitro for 10 d on control medium (containing 100 μM FeEDTA and 3 μM ZnSO_4) and transferred to Fe- or Zn-depleted media (without added Fe or Zn) for another 4 d before harvesting. GUS staining was performed overnight at 37°C in 50 mM PO_4^{2-} buffer pH 7.2, using 10 mM X-GLUC (5-bromo-4-chloro-3-indoxyl- β -D-glucuronid acid) (EUROMEDEX, Mundolsheim, France) as a substrate. Stained plants were either photographed or embedded in Technovit 7100 (Heraeus-Kulzer, Wehrheim, Germany) and cut in 5 μm sections using a Leica RM 2165 (Wetzlar, Germany) microtome. Prior to the observation using an Olympus BH2 microscope (Tokyo, Japan), sections were counterstained with the Schiff dye.

Enzymatic GUS activity

Roots and shoots from plants of eight lines (grown as indicated above) were harvested separately and subsequently homogenized in liquid N₂. Total proteins were extracted in GUS extraction buffer (50 mM PO_4^{2-} , 5 mM dithiothreitol, 1 mM EDTA, 0.1% Triton X-100, 0.1% Na lauryl sarcosyl). GUS activity was measured fluorometrically using 1 mM MUG (4-methylumbelliferyl- β -D-glucuronide) (EUROMEDEX, Mundolsheim, France) as a substrate (Jefferson et al. 1987). The measured activity was corrected with the total protein content (Bradford 1976).

Preparation of metal-chelates

DMA was produced as described (von Wirén et al. 1996), and chemically synthesized NA (Miyakoshi et al. 2001) was kindly provided by Professor Takeshi Kitahara, University of Tokyo, Japan. Fe-DMA and Fe-NA were prepared as described in Schaaf et al. (2004). Cu(II)-NA was prepared like Fe(III)-NA, but NA was supplied in 2-fold excess.

Electrophysiological studies in *Xenopus laevis* oocytes

Capped cRNA was transcribed from pOO2-*ZmYSL1* and pOO2-*AtYSL2* in vitro using the mMessage mMachine kit (Ambion, Austin, TX, USA), after linearization of plasmids with *Eco72I* and *MluI*, respectively. Metal-chelate-induced currents in oocytes were detected by two-electrode voltage clamp 3 d after cRNA injection. Oocyte experiments were essentially conducted as described in Schaaf et al. (2004).

Acknowledgments

We would like to thank Annegret Honsbein and Sabine Rauch for their excellent help with plant cultivation as well as Northern analysis,

and we gratefully acknowledge provision of the pFL61-AtYSL2 cDNA by Dr. E.L. Walker, Massachusetts, and of NA by S. Mori and T. Kitahara, Tokyo. We would also like to thank the anonymous reviewers for the constructive criticism and their encouragement during the review process of this paper. This study was supported by the Deutsche Forschungsgemeinschaft, Bonn, Germany, with a grant to N.v.W. (WI 1728/1 and 1728/6).

References

- Belouchi, A., Kwan, T. and Gros, P. (1997) Cloning and characterization of the OsNramp family from *Oryza sativa*, a new family of membrane proteins possibly implicated in the transport of metal ions. *Plant Mol. Biol.* 33: 1085–1092.
- Benes, I., Schreiber, K., Ripberger, H. and Kircheiss, A. (1983) Metal complex formation of nicotianamine, a possible phytosiderophore. *Experientia* 39: 261–262.
- Bourbouloux, A., Shahi, P., Chakladar, A., Delrot, S. and Bachhawat, A.K. (2000) Hgt1p, a high affinity glutathione transporter from the yeast *Saccharomyces cerevisiae*. *J. Biol. Chem.* 275: 13259–13265.
- Bradford, M.M. (1976) A rapid and sensitive method for the quantitation of microgram quantities of protein utilizing the principle of protein–dye binding. *Anal. Biochem.* 72: 248–254.
- Briat, J.F. and Lebrun, M. (1999) Plant responses to metal toxicity. *CR Acad. Sci. III* 322: 43–54.
- Briat, J.F. and Lobréaux, S. (1997) Iron transport and storage in plants. *Trends Plant Sci.* 2: 187–193.
- Bughio, N., Yamaguchi, H., Nishizawa, N.K., Nakanishi, H. and Mori, S. (2002) Cloning an iron-regulated metal transporter from rice. *J. Exp. Bot.* 53: 1677–1682.
- Catoni, E., Schwab, R., Hilpert, M., Desimone, M., Schwacke, R., Flugge, U.I., Schumacher, K. and Frommer, W.B. (2003) Identification of an *Arabidopsis* mitochondrial succinate–fumarate translocator. *FEBS Lett.* 534: 87–92.
- Chung, W.S., Lee, S.H., Kim, J.C., Heo, W.D., Kim, M.C., et al. (2000) Identification of a calmodulin-regulated soybean Ca(2+)-ATPase (SCA1) that is located in the plasma membrane. *Plant Cell* 12: 1393–1407.
- Clough, S.J. and Bent, A.F. (1998) Floral dip: a simplified method for *Agrobacterium*-mediated transformation of *Arabidopsis thaliana*. *Plant J.* 16: 735–743.
- Connolly, E.L., Campbell, N.H., Grotz, N., Prichard, C.L. and Guerinot, M.L. (2003) Overexpression of the FRO2 ferric chelate reductase confers tolerance to growth on low iron and uncovers posttranscriptional control. *Plant Physiol.* 133: 1102–1110.
- Connolly, E.L., Fett, J.P. and Guerinot, M.L. (2002) Expression of the *IRT1* metal transporter is controlled by metals at the levels of transcript and protein accumulation. *Plant Cell* 14: 1347–1357.
- Curie, C., Alonso, J.M., Le Jean, M., Ecker, J.R. and Briat, J.F. (2000) Involvement of NRAMP1 from *Arabidopsis thaliana* in iron transport. *Biochem. J.* 347: 749–755.
- Curie, C. and Briat, J.F. (2003) Iron transport and signaling in plants. *Annu. Rev. Plant Biol.* 54: 183–206.
- Curie, C., Panaviene, Z., Loulergue, C., Dellaporta, S.L., Briat, J.F. and Walker, E.L. (2001) Maize *yellow stripe1* encodes a membrane protein directly involved in Fe(III) uptake. *Nature* 409: 346–349.
- Dancis, A., Yuan, D.S., Haile, D., Askwith, C., Eide, D., Moehle, C., Kaplan, J. and Klausner, R.D. (1994) Molecular characterization of a copper transport protein in *S. cerevisiae*: an unexpected role for copper in iron transport. *Cell.* 76: 393–402.
- DiDonato, R.J., Jr, Roberts, L.A., Sanderson, T., Eisle, R.B. and Walker E.L. (2004) *Arabidopsis yellow stripe-like2* (YSL2): a metal-regulated gene encoding a plasma membrane transporter of nicotianamine–metal complexes. *Plant J.* 39: 403–414.
- Eide, D., Broderius, M., Fett, J. and Guerinot, M.L. (1996) A novel iron-regulated metal transporter from plants identified by functional expression in yeast. *Proc. Natl Acad. Sci. USA* 93: 5624–5628.
- Eyal, Y., Curie, C. and McCormick, S. (1995) Pollen specificity elements reside in 30 bp of the proximal promoters of two pollen-expressed genes. *Plant Cell* 7: 373–384.
- Gaymard, F., Pilot, G., Lacombe, B., Bouchez, D., Bruneau, D., Boucherez, J., Michaux-Ferriere, N., Thibaud, J. and Sentenac, H. (1998) Identification and disruption of a plant shaker-like outward channel involved in K⁺ release into the xylem sap. *Cell* 94: 647–655.
- Gazzarrini, S., Lejay, L., Gojon, A., Ninnemann, O., Frommer, W.B. and von Wirén, N. (1999) Three functional transporters for constitutive, diurnally regulated, and starvation-induced uptake of ammonium into *Arabidopsis* roots. *Plant Cell* 11: 937–948.
- Geisler, M., Frangne, N., Gomes, E., Martinoia, E. and Palmgren, M.G. (2000) The *ACA4* gene of *Arabidopsis* encodes a vacuolar membrane calcium pump that improves salt tolerance in yeast. *Plant Physiol.* 124: 1814–1827.
- Gietz, D., St Jean, A., Woods, R.A. and Schiestl, R.H. (1992) Improved method for high efficiency transformation of intact yeast cells. *Nucleic Acids Res.* 20: 1425.
- Guerinot, M.L. and Yi, Y. (1994) Iron: nutritious, noxious, and not readily available. *Plant Physiol.* 104: 815–820.
- Hamburger, D., Rezzonico, E., MacDonald-Comber Petetot, J., Somerville, C. and Poirier, Y. (2002) Identification and characterization of the *Arabidopsis* PHO1 gene involved in phosphate loading to the xylem. *Plant Cell* 14: 889–902.
- Harper, J.F., Hong, B., Hwang, I., Guo, H.Q., Stoddard, R., Huang, J.F., Palmgren, M.G. and Sze, H. (1998) A novel calmodulin-regulated Ca²⁺-ATPase (ACA2) from *Arabidopsis* with an N-terminal autoinhibitory domain. *J. Biol. Chem.* 273: 1099–1106.
- Higuchi, K., Suzuki, K., Nakanishi, H., Yamaguchi, H., Nishizawa, N.K. and Mori, S. (1999) Cloning of nicotianamine synthase genes, novel genes involved in the biosynthesis of phytosiderophores. *Plant Physiol.* 119: 471–480.
- Hoyos, M.E., Palmieri, L., Wertin, T., Arrigoni, R., Polacco, J.C. and Palmieri, F. (2003) Identification of a mitochondrial transporter for basic amino acids in *Arabidopsis thaliana* by functional reconstitution into liposomes and complementation in yeast. *Plant J.* 33: 1027–1035.
- Hwang, I., Sze, H. and Harper, J.F. (2000) A calcium-dependent protein kinase can inhibit a calmodulin-stimulated Ca²⁺ pump (ACA2) located in the endoplasmic reticulum of *Arabidopsis*. *Proc. Natl Acad. Sci. USA* 97: 6224–6229.
- Inoue, H., Higuchi, K., Nakanishi, H., Mori, S. and Nishizawa, N.K. (2003) Three rice nicotianamine synthase genes, OsNAS1, OsNAS2 and OsNAS3, are expressed in cells involved in long-distance transport of iron and differentially regulated by iron. *Plant J.* 36: 366–381.
- Jefferson, R.A., Kavanagh, T.A. and Bevan, M.W. (1987) GUS fusions: beta-glucuronidase as a sensitive and versatile gene fusion marker in higher plants. *EMBO J.* 13: 3901–3907.
- Kawai, S., Kamei, S., Matsuda, Y., Ando, R., Kondo, S., Ishizawa, A. and Alam, S. (2001) Concentrations of iron and phytosiderophores in xylem sap of iron-deficient barley plants. *Soil Sci. Plant Nutr.* 47: 265–272.
- Kim, E.J., Zhen, R.G. and Rea, P.A. (1994) Heterologous expression of plant vacuolar pyrophosphatase in yeast demonstrates sufficiency of the substrate-binding subunit for proton transport. *Proc. Natl Acad. Sci. USA* 91: 6128–6132.
- Lejay, L., Gansel, X., Cerezo, M., Tillard, P., Muller, C., Krapp, A., von Wirén, N., Daniel-Vedele, F. and Gojon, A. (2003) Regulation of root ion transporters by photosynthesis: functional importance and relation with hexokinase. *Plant Cell* 15: 2218–2232.
- Lejay, L., Tillard, P., Lepetit, M., Olive, F., Filleur, S., Daniel-Vedele, F. and Gojon, A. (1999) Molecular and functional regulation of two NO₃⁻ uptake systems by N- and C-status of *Arabidopsis* plants. *Plant J.* 18: 509–519.
- Liu, G., Sanchez-Fernandez, R., Li, Z.S. and Rea, P.A. (2001) Enhanced multi-specificity of *Arabidopsis* vacuolar multidrug resistance-associated protein-type ATP-binding cassette transporter, AtMRP2. *J. Biol. Chem.* 276: 8648–8656.
- Lubkowitz, M.A., Barnes, D., Breslav, M., Burchfield, A., Naider, F. and Becker, J.M. (1998) *Schizosaccharomyces pombe isp4* encodes a transporter representing a novel family of oligopeptide transporters. *Mol. Microbiol.* 28: 729–741.
- Ludwig, U., von Wirén, N. and Frommer, W.B. (2002) Uniport of NH₄⁺ by the root hair plasma membrane ammonium transporter LeAMT1;1. *J. Biol. Chem.* 277: 13548–13555.
- Malmström, S., Akerlund, H.E. and Askerlund, P. (2000) Regulatory role of the N terminus of the vacuolar calcium-ATPase in cauliflower. *Plant Physiol.* 122: 517–526.

- Mäser, P., Thomine, S., Schroeder, J.I., Ward, J.M., Hirschi, K., et al. (2001) Phylogenetic relationships within cation transporter families of *Arabidopsis*. *Plant Physiol.* 126: 1646–1667.
- Miyakoshi, K., Oshita, J. and Kitahara, T. (2001) Expedient synthesis of nicotianamine and 2'-deoxymugineic acid. *Tetrahedron* 57: 3355–3360.
- Mizuno, D., Higuchi, K., Sakamoto, T., Nakanishi, H., Mori, S. and Nishizawa, N.K. (2003) Three nicotianamine synthase genes isolated from maize are differentially regulated by iron nutritional status. *Plant Physiol.* 132: 1989–1997.
- Mori, S., Nishizawa, N., Kawai, S., Sato, Y. and Takagi, S. (1987) Dynamic state of mugineic acid and analogous phytosiderophores in Fe-deficient barley. *J. Plant Nutr.* 10: 1003–1011.
- Pich, A., Manteuffel, R., Hillmer, S., Scholz, G. and Schmidt, W. (2001) Fe homeostasis in plant cells: does nicotianamine play multiple roles in the regulation of cytoplasmic Fe concentration? *Planta* 213: 967–976.
- Pich, A., Scholz, G. and Stephan, U.W. (1994) Iron dependent changes of heavy metals, nicotianamine, and citrate in different plant organs and in the xylem exudate of two tomato genotypes. Nicotianamine as possible copper translocator. *Plant Soil* 165: 189–196.
- Pittman, J.K. and Hirschi, K.D. (2001) Regulation of CAX1, an *Arabidopsis* Ca²⁺/H⁺ antiporter. Identification of an N-terminal autoinhibitory domain. *Plant Physiol.* 127: 1020–1029.
- Pittman, J.K., Sreevidya, C.S., Shigaki, T., Ueoka-Nakanishi, H. and Hirschi, K.D. (2002) Distinct N-terminal regulatory domains of Ca²⁺/H⁺ antiporters. *Plant Physiol.* 130: 1054–1062.
- Rentsch, D., Laloi, M., Rouhara, I., Schmelzer, E., Delrot, S. and Frommer, W.B. (1995) *NTRI* encodes a high affinity oligopeptide transporter in *Arabidopsis*. *FEBS Lett.* 370: 264–268.
- Robinson, N.J., Procter, C.M., Connolly, E.L. and Guerinot, M.L. (1999) A ferric-chelate reductase for iron uptake from soils. *Nature* 397: 694–697.
- Rose, M.D., Winston, F. and Hieter, P. (1990) *Methods in Yeast Genetics*. Cold Spring Harbor Laboratory Press, Cold Spring Harbor, NY.
- Römheld, V. and Marschner, H. (1986) Mobilization of iron in the rhizosphere of different plant species. In *Advances in Plant Nutrition*, Vol. 2. Edited by Tinker, B. and Läuchli, A. pp. 155–204. Praeger Scientific, New York.
- Sambrook, J., Fritsch, E.F. and Maniatis, T. (1989) *Molecular Cloning: A Laboratory Manual*. Cold Spring Harbor Laboratory Press, Cold Spring Harbor, NY.
- Schaaf, G., Catoni, E., Fitz, M., Schwacke, R., Schneider, A., von Wirén, N. and Frommer, W.B. (2002) A putative role for the vacuolar calcium/manganese proton antiporter AtCAX2 in heavy metal detoxification. *Plant Biol.* 4: 612–618.
- Schaaf, G., Ludewig, U., Erenoglu, B.E., Mori, S., Kitahara, T. and von Wirén, N. (2004) ZmYS1 functions as a proton-coupled symporter for phytosiderophore- and nicotianamine-chelated metals. *J. Biol. Chem.* 279: 9091–9096.
- Schmidt, W. (2003) Iron solutions: acquisition strategies and signaling pathways in plants. *Trends Plant Sci.* 8: 188–193.
- Spizzo, T., Byersdorfer, C., Duesterhoeft, S. and Eide, D. (1997) The yeast *FET5* gene encodes a *FET3*-related multicopper oxidase implicated in iron transport. *Mol. Gen. Genet.* 256: 547–556.
- Stephan, U.W., Schmidke, I., Stephan, V.W. and Scholz, G. (1996) The nicotianamine molecule is made-to-measure for complexation of metal micronutrients in plants. *Biometals* 9: 84–90.
- Stephan, U.W. and Scholz, G. (1993) Nicotianamine—mediator of transport of iron and heavy-metals in the phloem? *Physiol. Plant.* 88: 522–529.
- Takahashi, M., Terada, Y., Nakai, I., Nakanishi, H., Yoshimura, E., Mori, S. and Nishizawa, N.K. (2003) Role of nicotianamine in the intracellular delivery of metals and plant reproductive development. *Plant Cell* 15: 1263–1280.
- Takahashi, M., Yamaguchi, H., Nakanishi, H., Shioiri, T., Nishizawa, N.K. and Mori, S. (1999) Cloning two genes for nicotianamine aminotransferase, a critical enzyme in iron acquisition (strategy II) in graminaceous plants. *Plant Physiol.* 121: 947–956.
- Takano, J., Noguchi, K., Yasumori, M., Kobayashi, M., Gajdos, Z., Miwa, K., Hayashi, H., Yoneyama, T. and Fujiwara, T. (2002) *Arabidopsis* boron transporter for xylem loading. *Nature* 420: 337–340.
- Thomine, S., Lelievre, F., Debarbieux, E., Schroeder, J.I. and Barbier-Brygoo, H. (2003) AtNRAMP3, a multispecific vacuolar metal transporter involved in plant responses to iron deficiency. *Plant J.* 34: 685–695.
- Thomine, S., Wang, R., Ward, J.M., Crawford, N.M. and Schroeder, J.I. (2000) Cadmium and iron transport by members of a plant metal transporter family in *Arabidopsis* with homology to *Nramp* genes. *Proc. Natl Acad. Sci. USA* 97: 4991–4996.
- Thompson, J.D., Higgins, D.G. and Gibson, T.J. (1994) CLUSTAL W: improving the sensitivity of progressive multiple sequence alignment through sequence weighting, position-specific gap penalties and weight matrix choice. *Nucleic Acids Res.* 22: 4673–4680.
- Tiffin, L.O. (1965) Iron translocation. plant culture, exudate sampling, iron citrate analysis. *Plant Physiol.* 41: 510–514.
- Vacchina, V., Mari, S., Czernic, P., Marques, L., Pianelli, K., Schaumlöffel, D., Lebrun, M. and Lobinski, R. (2003) Speciation of nickel in a hyperaccumulating plant by high-performance liquid chromatography inductively coupled plasma mass spectrometry and electrospray MS/MS assisted by cloning using yeast complementation. *Anal. Chem.* 75: 2740–2745.
- Vert, G., Briat, J.F. and Curie, C. (2001) *Arabidopsis* *IRT2* gene encodes a root-periphery iron transporter. *Plant J.* 26: 181–189.
- Vert, G.A., Briat, J.F. and Curie, C. (2003) Dual regulation of the *Arabidopsis* high-affinity root iron uptake system by local and long-distance signals. *Plant Physiol.* 132: 796–804.
- Vert, G., Grotz, N., Dédaldéchamp, F., Gaymard, F., Guerinot, M.L., Briat, J.F. and Curie, C. (2002) *IRT1*, an *Arabidopsis* transporter essential for iron uptake from the soil and for plant growth. *Plant Cell* 14: 1223–1233.
- von Wirén, N., Klair, S., Bansal, S., Briat, J.F., Khodr, H., Shioiri, T., Leigh, R.A. and Hider, R.C. (1999) Nicotianamine chelates both Fe^{III} and Fe^{II}. Implications for metal transport in plants. *Plant Physiol.* 119: 1107–1114.
- von Wirén, N., Marschner, H. and Römheld, V. (1996) Roots of iron-efficient maize also absorb phytosiderophore-chelated zinc. *Plant Physiol.* 111: 1119–1125.
- von Wirén, N., Mori, S., Marschner, H. and Römheld, V. (1994) Iron inefficiency in maize mutant *ys1* (*Zea mays* L. cv *Yellow-Stripe*) is caused by a defect in uptake of iron phytosiderophores. *Plant Physiol.* 106: 71–77.
- Wei, J. and Theil, E.C. (2000) Identification and characterization of the iron regulatory element in the ferritin gene of a plant (soybean). *J. Biol. Chem.* 275: 17488–17493.
- Zaharieva, T. and Römheld, V. (2001) Specific Fe²⁺ uptake system in strategy I plants inducible under Fe deficiency. *J. Plant Nutr.* 23: 1733–1744.

(Received June 11, 2004; Accepted February 25, 2005)